Electronic and optical properties of unstrained and strained wurtzite GaN

Zhongqin Yang
Surface Physics Laboratory, Fudan University, Shanghai 200433, China
and Fudan–T. D. Lee Physics Laboratory, Fudan University, Shanghai 200433, China

Zhizhong Xu
China Center of Advanced Science and Technology (World Laboratory), P.O. Box 8730, Beijing 100080, China;
Surface Physics Laboratory, Fudan University, Shanghai 200433, China;
and Fudan–T. D. Lee Physics Laboratory, Fudan University, Shanghai 200433, China
(Received 24 June 1996; revised manuscript received 26 August 1996)

A semiempirical tight-binding method in the sp^3s^* model is used to investigate the electronic and optical properties of strained and unstrained wurtzite GaN (α-GaN). The calculated unstrained fundamental gap of α-GaN is 3.45 eV, which is in agreement with experiment. The empirical scaling rule has been used in the strained band-structure calculation, where the strains cover −5–5 %. The band gap at the Γ point increases with the absolute value of strains. GaN has an indirect band gap when strains reach 5%. The unstrained and strained density of states and imaginary part of the dielectric function $[\epsilon_2(\omega)]$ are studied. There are mainly three peaks at 6.4, 7.5, and 8.4 eV dominating the unstrained $\epsilon_2(\omega)$ spectrum, whose two components, $\epsilon_{2xy}(\omega)$ and $\epsilon_{2z}(\omega)$, are also calculated. Both the shape and energy position of the peaks of the $\epsilon_2(\omega)$ successively change with the strains. The real part of the dielectric function, reflectivity, refractive index, and the effects of the strains on them are all researched. [S0163-1829(96)10448-3]

I. INTRODUCTION

The development in the past decade of light-emitting diodes and semiconductor lasers operating in the red-to-green spectral region and the aim to realize full-color display systems has prompted the search for devices operating in the blue-ultraviolet (uv) energy range. GaN, especially, wurtzite GaN (α-GaN) is a promising candidate for the fabrication of such devices, since it possesses a direct gap in the near uv (around 3.4 eV), is resistant to radiation damage, and can form solid solutions with InN and AlN, which permits the tailoring of its optical and electrical behavior.[1] The latest applications of α-GaN in optical and microelectronic structures involve device-quality contacts,[2] uv photoconductors,[3] InGaN/GaN and AlGaN/GaN double-heterostructure uv-blue light-emitting diodes (LED's),[4] etc. The making of these devices is largely based on the profound research on the electronic and optical properties of α-GaN.

It is reported that the deposition of α-GaN has been successful on various substrates, such as Si(111),[5] sapphire at various orientations [mainly (0001)], but also $(01\bar{1}2)$,[6] $(11\bar{2}0)$,[5] and $(1\bar{1}02)$,[7] GaAs(111),[8] as well as on 6HSiC(0001).[9] Unfortunately, neither the lattice nor the thermal expansion of those substrates match well with α-GaN's. To do further research on α-GaN, it is necessary to examine the properties of strained GaN.

Due to the complexity of wurtzite over zinc-blende GaN (β-GaN), there have been relatively few theoretical studies of α-GaN (Refs. 10–13) until recently. And among those few theoretical studies, most calculated band structures; the properties of α-GaN have seldom been considered.

In this work, we present the electronic and optical properties of unstrained and strained α-GaN using the nearest and second-nearest-neighbor semiempirical tight-binding (SETB) approach in the sp^3s^* model. The density of states (DOS) and the imaginary part of the dielectric function $[\epsilon_2(\omega)]$ are the most important parameters in solid-state physics, which have been researched first in the optical properties calculation. Since α-GaN is anisotropic, it is necessary to research $\epsilon_2(\omega)$ in two components, the in-plane component $\epsilon_{2xy}(\omega)$, which is the average over the X and Y direction, and the Z component and $\epsilon_{2z}(\omega)$, which is perpendicular to $\epsilon_{2xy}(\omega)$. They are both calculated. Using the Kramers-Kronig relations, the real part of the dielectric function $[\epsilon_1(\omega)]$ is derived from $\epsilon_2(\omega)$. We also study the features of some very useful optical constants, including reflectivity (R), the absorption coefficient (α), and refractive index (n). In Sec. II, the calculated methods are described. The results, discussions, and analyses are presented in Sec. III. Section IV gives the summary.

II. CALCULATION

A. Unstrained and strained band structures

There are two anions (nitrogen) and two cations (gallium) in an α-GaN unit cell. We adopt the semiempirical tight-binding theory developed by Vogl *et al.*,[14] considering the nearest- and second-nearest-neighbor interactions. An sp^3s^* basis centered at each of the four atomic sites per unit cell is used, which leads to a 20×20 Hamiltonian. The number of nonzero tight-binding parameters is limited to one-center on-site integrals, nearest-, and second-nearest-neighbor two-center integrals, as discussed by Slater and Koster.[15] For the second-nearest neighbors, only interactions between the s^* orbital and the three p orbitals are considered. Thus our model has 15 independent parameters: the six on-site matrix elements $E(s,a)$, $E(s^*,a)$, $E(p,a)$, $E(s,c)$, $E(s^*,c)$, and $E(p,c)$ [where s and p refer to the basis states and a and c

 © 1996 The American Physical Society

TABLE I. The fitted nearest- and second-nearest-neighbor tight-binding parameters of α-GaN (eV).

$E(s,a)$	$E(s^*,a)$	$E(p,a)$	$E(s,c)$	$E(s^*,c)$	$E(p,c)$	$V(ss\sigma)$	
12.86	3.437	7.603	−1.059	10.17	0.0028	5.660	
$V(sp\sigma)$	$V(ps\sigma)$	$V(pp\pi)$	$V(pp\sigma)$	$V(s^*p\sigma)$	$V(ps^*\sigma)$	$V(s^*p,a)$	$V(s^*p,c)$
6.394	2.945	3.468	−1.594	4.889	−2.522	−0.2217	0.2122

refer to anion (N) and cation (Ga)]; the seven nearest-neighbor transfer-matrix elements $V(ss\sigma)$, $V(sp\sigma)$, $V(ps\sigma)$, $V(pp\pi)$, $V(pp\sigma)$, $V(s^*p\sigma)$, and $V(ps^*\sigma)$, [where the first (second) index refers to the N (Ga)]; and finally, two second-nearest-neighbor transfer-matrix elements $V(s^*p,a)$, $V(s^*p,c)$. All these parameters are determined by fitting the band structures with the theoretical calculation[13] and experiments.[16] The Ga $3d$ orbitals would have provided a better approximation; however, due to the calculation complexity, their contribution is neglected here.

The effects of strains on the energy band structures are embodied by modifying the SETB parameters according to the changes of bond lengths and angles. In these calculations, the changes of the second-neighbor parameters are neglected approximately and only the changes of the nearest-neighbor parameters are considered. The changes by the bond angles are calculated through the variations in the direction cosines,[17] and the changes by the bond lengths are determined by means of an empirical scaling rule of the following form:

$$V_{\alpha\beta}=V_{\alpha\beta}(0)(d/d_0)^{-n(\alpha\beta)}, \tag{1}$$

where $V_{\alpha\beta}$ and $V_{\alpha\beta}(0)$ are the strained and unstrained interaction parameters, and d and d_0 are the strained and unstrained interatomic distances. $n(\alpha\beta)$ is a scaling index, which, according to Harrison's rule,[18] is equal to 2 for all orbitals $(\alpha\beta)$. Since there is no decisive fundamental argument for or against the given scaling rule and the purpose of this work is to discuss the effects of the strains, the scaling indexes $n(\alpha\beta)$ are determined by fitting the deformation-potential constants (DPC's) with Christensen and Gorczyca's[19] values. They are given in Sec. III.

Since α-GaN has hexagonal symmetry, the elements of the strain tensor on the X-Y plane are equivalent. Namely, $e_1=e_2\equiv e_\parallel$ (where e_1, e_2 are the X, Y component of the strain tensor, respectively). And they are written as

$$e_\parallel=e_1=e_2=\frac{a_i-a}{a}, \tag{2}$$

where a and a_i are the lattice constants of the α-GaN and substrate, respectively, and a is 3.19 (Å) taken from.[16] In this paper, e_1 (e_2) is varied from −5% to 5%. When e_1 (e_2) is positive, the α-GaN grown on the substrate dilates; when e_1 (e_2) is negative, it compresses. e_3 ($e_\perp$) is the Z component of the strain tensor, which is expressed as

$$e_\perp=e_3=\frac{a_l-c}{c}, \tag{3}$$

where a_l is the strained lattice constant in the Z direction of α-GaN, and c is the unstrained one.

For hexagonal crystals, the Z component of the stress and the strain tensor are related by

$$\tau_3=C_{13}e_1+C_{13}e_2+C_{33}e_3, \tag{4}$$

where C_{13}, C_{33} are the elastic constants of α-GaN. They are taken as 15.8×10^{10} Pa and 26.7×10^{10} Pa, respectively. In the Z direction, there is no stress on the surface, so $\tau_3=0$. From formulas (2) and (4), we can obtain

$$e_\perp=\frac{-2C_{13}}{C_{33}}e_\parallel. \tag{5}$$

Considered formulas (3) and (5), the strained lattice constant in the Z direction (a_l) can be obtained as

$$a_l=c\left(1-\frac{2C_{13}}{C_{33}}e_\parallel\right). \tag{6}$$

In the ideal case, the c/a ratio equals $2\sqrt{6}/3$ and the internal bond-length parameter u (d_0/c) is 3/8. That is to say, $d_0=(\sqrt{6}/4)a$. In the calculation, it is assumed that the four interatomic distances still equal each other after strains. Through simple mathematical calculation, the strained interatomic distance (d) is written as follows:

$$d=\frac{a_l}{4}+\frac{a_i^2}{3a_l}. \tag{7}$$

B. DOS and optical constants

The DOS(ω) is expressed by the following:

$$\mathrm{DOS}(\omega)=\frac{2}{(2\pi)^3}\int\frac{ds}{|\Delta_k\epsilon(k)|}. \tag{8}$$

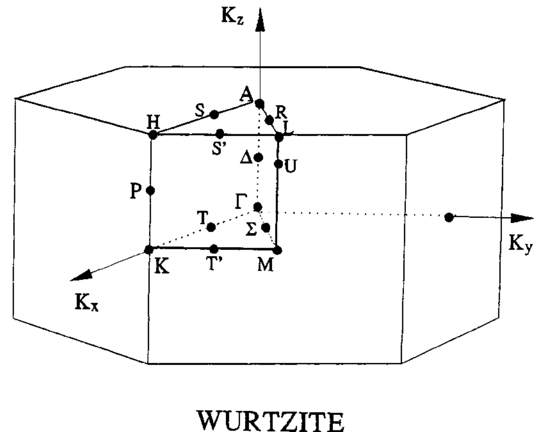

FIG. 1. Brillouin zone of wurtzite GaN.

TABLE II. The calculated critical-point energies of the major electronic transitions up to 9 eV of α-GaN. The energies of the experimental dielectric-function structures are also noted.

	Energy (eV)				
Transition	This work (SETB)	Huang and Ching (OLCAO)[a]	Gorczyca and Christensen (LMTO-LDA)[b]	Xu and Ching (OLCAO)[c]	Logothetidis *et al.* (Experiment)[d]
Γ_6-Γ_1	3.45	3.50	3.44	2.65	3.35
Γ_5-Γ_3	6.0	5.8	6.0	6.0	
M_4-M_1	6.03	7.05	7.03	6.7	7.0
M_4-M_3	7.2	7.3	7.4	7.25	7.0
H_3-H_3	7.8	8.4	8.8	8.5	7.9
M_2-M_1	8.6	8.5	8.7	8.6	7.9
K_2-K_3	8.0	9.05	9.5	9.0	9.0

[a]Orthogonalized linear combination of atomic orbitals (not self-consistent) with local-density-approximation (LDA) adjustment, Ref. 10.
[b]Linear muffin-tin-orbital method, with LDA adjustment, Ref. 24.
[c]Orthogonalized linear combination of atomic orbitals (self-consistent) without LDA adjustment, Ref. 25.
[d]α-GaN thin films grown on sapphire substrate, at room temperature, Ref. 23.

From the band structure of K space in the Brillouin zone (BZ), the DOS has been obtained by a numerical method, which is developed by Gilat and Raubenheimer.[20] The method involves dividing the irreducible section of the first BZ into a cubic mesh and approximating the constant-energy surfaces inside every small cube by a set of parallel planes; and perturbation is used to calculate the gradient of the equal-energy surface. We used 3552 K points in the irreducible part of the BZ. The DOS of α-GaN is calculated in the energy region -10–12 eV, neglecting the spin-orbital interaction.

At low temperature, the dielectric function of nonpolar crystal is determined mainly by the transition between the valence and conduction bands. According to perturbation theory, $\epsilon_2(\omega)$ is expressed as[21]

$$\epsilon_2(\omega)=\frac{4\pi^2e^2}{3m^2\omega^2}\sum_{l,n}\int_{\mathrm{BZ}}\frac{2}{(2\pi)^3}d^3k|P_{nl}|^2 \times\delta[E_l(k)-E_n(k)-\hbar\omega], \tag{9}$$

where m,e is the mass and electrical charge of the electron, respectively; $\Sigma_{l,n}$ means the summation between all the conduction bands (l) and valence bands (n); and P_{nl} expresses the momentum matrix element between l and n, which has been derived by Lew Yan Voon and Ram-Mohan[22] in the tight-binding representation. It is given by

$$P_{nl}=\frac{m}{\hbar}\langle nk|\nabla_kH(k)|lk\rangle \tag{10}$$

where $H(k)$ is the tight-binding Hamiltonian, and $\langle nk|,|lk\rangle$ are the K-space wave functions, which can be obtained by $H(k)$. So, with the 15 tight-binding parameters, we can directly calculate P_{nl}. In the strained cases, P_{nl} has the same formula. It changes only due to the Hamiltonian matrix elements. When calculating the integration of $\epsilon_2(\omega)$, we use the same method as used for the DOS. The calculation has been performed in the energy region 0.0–10 eV, and four conduction bands and three valence bands are involved.

The real part of the dielectric function $[\epsilon_1(\omega)]$ can be derived from $\epsilon_2(\omega)$ by the Kramers-Kronig relation. In our calculation, the relation is written as follows:

$$\epsilon_1(\omega)-1=\frac{2}{\pi}\lim_{\eta\to 0}\left[\int_0^{\omega-\eta}\frac{\omega'\epsilon_2(\omega')}{\omega'^2-\omega^2}d\omega' + \int_{\omega+\eta}^{\omega_c}\frac{\omega'\epsilon_2(\omega')}{\omega'^2-\omega^2}dw'\right] + \frac{2}{\pi}\int_{\omega_c}^{\infty}\frac{\omega'\epsilon_2(\omega')}{\omega'^2-\omega^2}d\omega', \tag{11}$$

where η and ω_c (E_c) are 0.0013 and 10.0 eV, respectively. When $\omega \geqslant \omega_c$, we make the approximation $\epsilon_2(\omega)\approx A/\omega^2$, where the constant A is obtained by $\epsilon_2(\omega_c)$: $A=\omega_c^2\epsilon_2(\omega_c)$. So the last term in (10) is therefore

$$\frac{2A}{\pi}\int_{\omega_c}^{\infty}\frac{d\omega'}{(\omega')(\omega'^2-\omega^2)}=-\frac{\omega_c^2\epsilon_2(\omega_c)}{\pi\omega^2}\ln\left(1-\frac{\omega^2}{\omega_c^2}\right). \tag{12}$$

The refractive index (n) and reflectivity (R) have been obtained by the following formulas (where k is the extinction coefficient):

$$n=\left[\frac{\sqrt{\epsilon_1^2+\epsilon_2^2}+\epsilon_1}{2}\right]^{1/2}, \tag{13}$$

$$k=\left[\frac{\sqrt{\epsilon_1^2+\epsilon_2^2}-\epsilon_1}{2}\right]^{1/2}. \tag{14}$$

If light is reflected at near-normal incidence at the surface of a sufficiently thick crystal, such that the transmission can be neglected, the reflectivity (R) is given by

$$R=\frac{(n-1)^2+k^2}{(n+1)^2+k^2}. \tag{15}$$

III. RESULTS AND DISCUSSION

A. Band structures and DOS

The 15 tight-binding parameters of Table I are determined by fitting band structures[13,16] at the Γ, A, H, L, K, and M points of the Brillouin zones. (The BZ of the α-GaN is

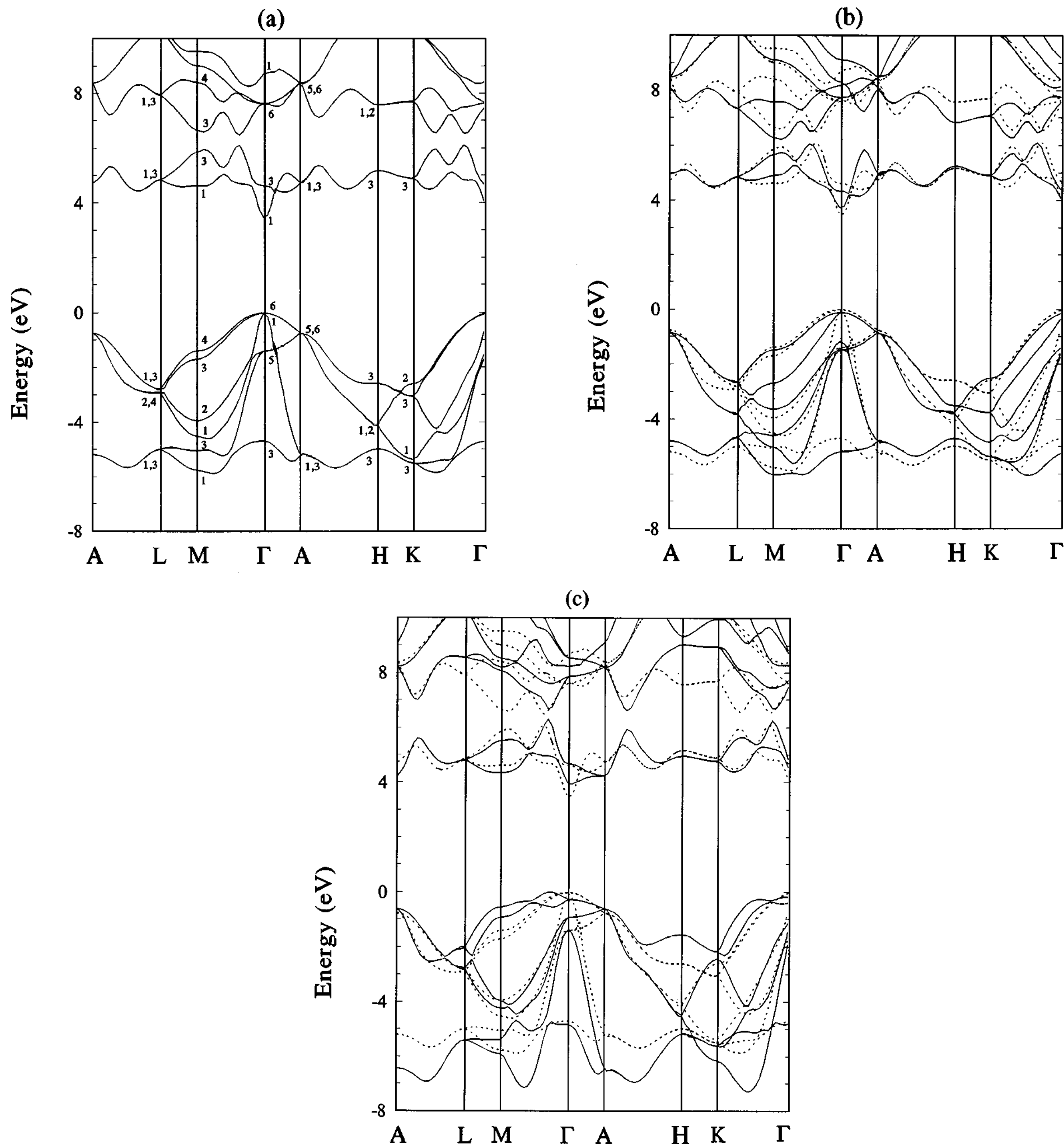

FIG. 2. Band structure (a) of unstrained α-GaN, and (b) under strains of -5% and (c) 5%. The dotted lines in (b) and (c) represent the unstrained results.

shown in Fig. 1 with high symmetric points indicated.) Some fitted energy gaps of those high-symmetry points are listed in Table II, where the present results are compared with previously reported band structures (Huang and Ching,[10] Logothetidis *et al.*,[23] Gorczyca and Christensen,[24] and Xu and Ching[25]). (The ''transition'' in Table II refers to the band transition energy between the upper valence and lower conduction bands.) The results are in agreement with each other; especially, our fundamental gap of Γ is direct and 3.45 eV, which agrees well with the previous experimental data.[16] Figure 2(a) shows the unstrained α-GaN structure along high symmetrical lines of the Brillouin Zone obtained by our fitting procedure.

As in nearly all tight-binding models, the valence bands in Fig. 2(a), which are mainly derived from the N $2p$ state with a sizable mixture of Ga $4s$ and $4p$ states, are reproduced accurately. The lowest conduction band is also well reproduced and is composed primarily of the Ga $4s$ state. The upper conduction bands are primarily of Ga $4p$ character and are less accurately reproduced. Fortunately these are the least important bands in the problems concerning the band transition.

Our calculation shows that, just as pointed out by Priester *et al.*,[26] the scaling indexes are only connected with hydrostatic DPC's and have no dependence on shear DPC's; so $n(\alpha\beta)$ are determined only by fitting the hydrostatic DPC's,

TABLE III. The sealing indexes $n(\alpha\beta)$ for wurtzite GaN.

$(\alpha\beta)$	(ss)	(sp)	(ps)	$(pp\sigma)$	$(pp\pi)$	(s^*p)	(ps^*)
$n(\alpha\beta)$	4.98	15.63	4.29	11.06	−16.4	−8.0	−1.69

and all the strains in the X, Y, and Z directions are taken as 0.001. The deformation-potential constants used here are given by Christensen and Gorczyca[19] (with the linear muffin-tin-orbital method).

Table III is the fitted indexes $n(\alpha\beta)$ for α-GaN. We should point out that the determination of indexes is not unique. A set of indexes is selected to match as well as possible for most DPC's in the calculation. The deformation-potential constants calculated with the fitted $n(\alpha\beta)$ are listed in Table IV.

The strained band structures are showed in Fig. 2 with $e_{\parallel}$ strains of −5% (b) and 5% (c) each compared to the unstrained band structure (dotted line). It is found that the fundamental gap at the Γ point grows with the increase of the absolute value of strains. The variation of this energy gap with strains is shown in Fig. 3. The energy gap varies nearly linearly with strains. This tendency is identical with the experiment measured by Perlin *et al.*[27]

In Fig. 2(c), the top of the valence band is not at Γ, but at the left of Γ. And the bottom of the conduction band displaces in the right-hand direction. That is to say, when the strains reach 5%, α-GaN turns out to be an indirect band structure. On the other hand, when the strains are negative, there is no corresponding result. With the −5% strains, as shown in Fig. 2(b), the top of the valence band and the bottom of the conduction band are still located at Γ; the band gap, however, grows up to 3.90 eV. It may be too wide for blue light-emitting devices and other applications, so trying to decrease strains is necessary.

The DOS of unstrained α-GaN is given in Fig. 4. Compared with the results of Huang and Ching[10] shown in the inset of Fig. 4, both spectra have the same principal peaks in the corresponding regions, although the positions and heights of the peaks are not in complete agreement. The figure also shows that the direct band gap of the α-GaN is about 3.45 eV.

Figure 5 displays the strained density of states for α-GaN, which is compared with the unstrained DOS's (dotted lines). The DOS's of conduction bands vary slowly with the strains. When strains are 5%, the difference between the strained and unstrained DOS's of valence bands is very great; however, for −5%, the difference is not as much. It can be concluded that positive strains have a greater effect on DOS's than negative strains. So it may be the positive strains that should be tried to reduce first.

TABLE IV. The deformation-potential constants of wurtzite GaN. The row labeled "Calc." gives the values obtained in this paper, and the "Theor." row gives the values of Christensen and Gorczyca.

	Γ_v-Γ_c	Γ_v-A_c	Γ_v-L_c	Γ_v-M_c	Γ_v-H_c	Γ_v-K_c
Calc.	−8.32	−7.57	−3.41	−3.45	−4.59	−0.83
Theor.	−7.8	−7.2	−3.4	−2.8	−3.2	0.36

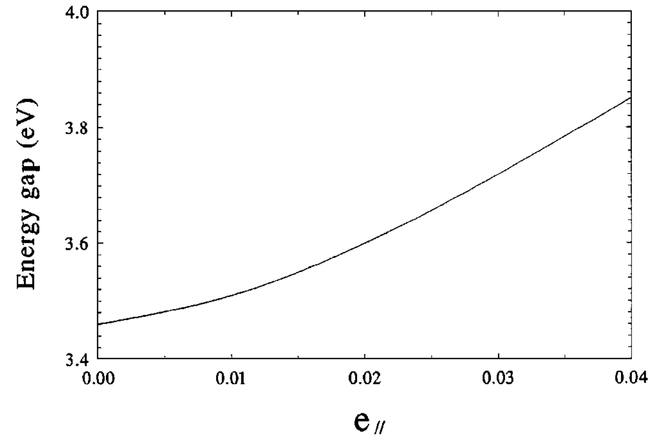

FIG. 3. Energy gap between valence and conduction bands at Γ of α-GaN under strains from 0.0% to 4.0%.

B. Optical properties

Figure 6 is our unstrained results of the imaginary part of the dielectric function $\epsilon_2(\omega)$, and the insets are the results of Christensen and Gorczyca, using the self-consistent linear muffin-tin-orbital method.[19] Comparing our results with theirs in Figs. 6(a) and 6(b), the spectra have some features in common. In the 6–9-eV photon energy range, there are three peaks of either $\epsilon_{2xy}(\omega)$ or $\epsilon_{2z}(\omega)$. In Fig. 6(b), the inset's highest of the three $\epsilon_{2z}(\omega)$ peaks is on the left, which is the same as ours. And the corresponding photon energies are both about 6.4 eV. In our case, this $\epsilon_{2z}(\omega)$ peak decides the highest E_1^* peak of the average $\epsilon_2(\omega)$ peaks in Fig. 6(c). In Fig. 6(d), we present our calculated unstrained real and imaginary part of the dielectric function, compared with the experimental data (which, to our knowledge, is unique). In the 0.0–10.0-eV photon energy range, there are mainly three peaks at 6.4, 7.5, and 8.4 eV, denoted E_1^*, E_2^*, and E_3^*, respectively, in Fig. 6(a); and the experimental data are 7.0, 7.9, and 9.0 eV (see Table II). The three peaks of Chris-

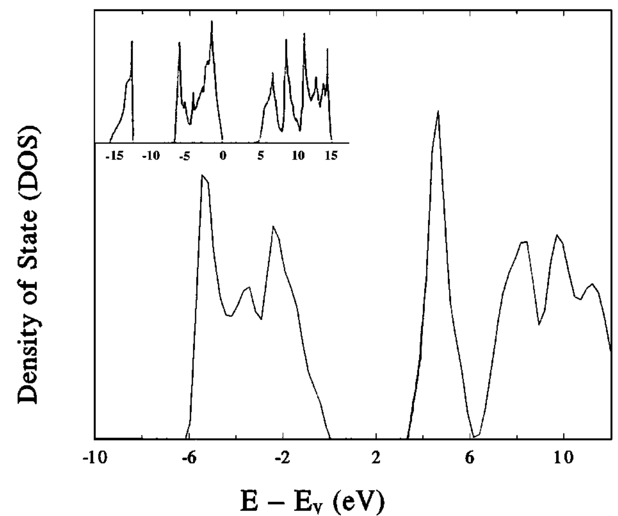

FIG. 4. The total DOS for bulk α-GaN without strains, compared with the result of Huang and Ching (inset) with a minimal basis semi-*ab initio* approach.

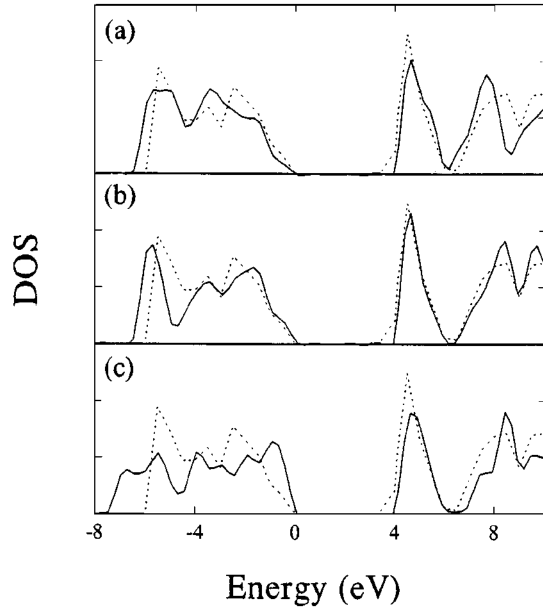

FIG. 5. The total density of states (DOS) of α-GaN (full line) under strains of (a) -5%, (b) 1%, and (c) 5%. The dotted lines represent the unstrained results.

tensen and Gorczyca are located at 6.1, 6.9, and 7,9 eV. Our results seem better than theirs.

Referring to Table II, the three distinct structures E_1^*, E_2^*, and E_3^* can be assigned to the transition of the specific points in the BZ. The Γ_5-Γ_3 transition energy is around 6.0 eV, and the M_4-M_1 transition occurs at energies between 6.03 and 7.05 eV, obtained by different researchers. These two interband excitations are thought to compose the first structure (E_1^*, 6.4 eV). The second structure (E_2^*, 7.5 eV) could be related to the M_4-M_3 transition, which is reported to take place from 7.0 to 7.4 eV, and possibly to the H point (H_3-H_3) that covers a broad energy range (from Table II). The gaps of the M_2-M_1 and K_2-K_3 transitions are close to 8.4 eV, so they may be responsible for the third feature E_3^* (8.4 eV).

The strains make both the shape and the position of the main peaks of $\epsilon_2(\omega)$ vary successively. When the strains are small (about $\pm 1\%$), $\epsilon_2(\omega)$ is very similar to the unstrained $\epsilon_2(\omega)$. While the strains are equal to $\pm 4\%$, there are two high peaks in the $\epsilon_2(\omega)$ diagram. The results of the 1% and 4% strains are shown in Fig. 7, compared with the unstrained curve (dotted). The real part of dielectric function $[\epsilon_1(\omega)]$ also varies obviously under the strains.

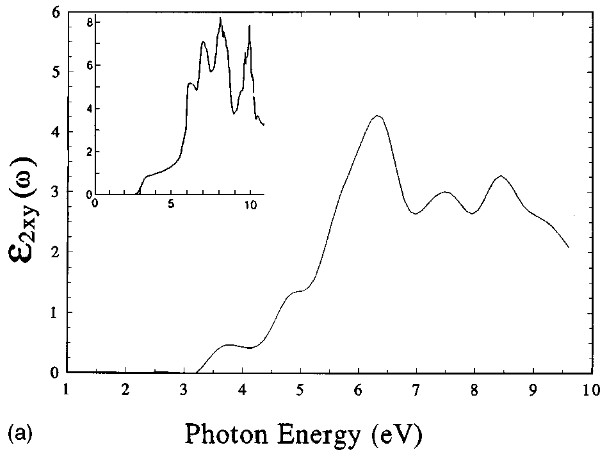

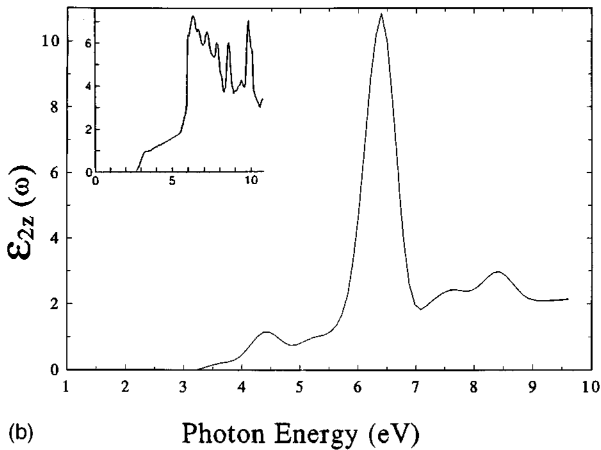

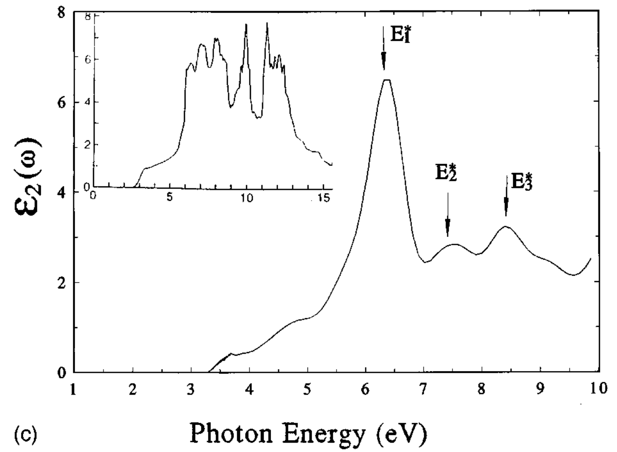

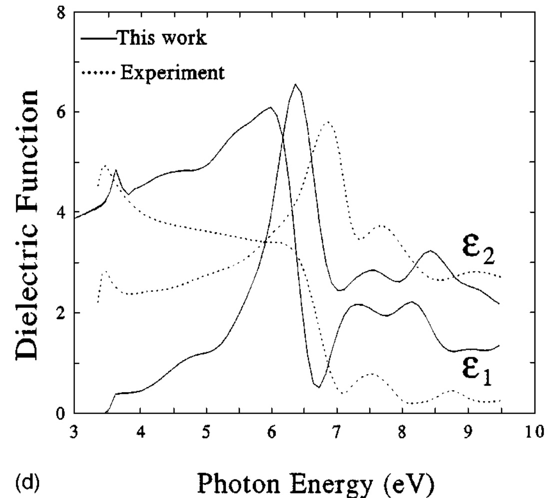

FIG. 6. The imaginary part of the dielectric function $[\epsilon_2(\omega)]$ of α-GaN (no strain). (a) Polarization in the XY plane, (b) polarization along the Z axis, and (c) average value over the three directions. Their insets are the results of Christensen and Gorczyca (d). The real (ϵ_1) and imaginary (ϵ_2) parts of the dielectric function of α-GaN compared with the experimental data (no strain).

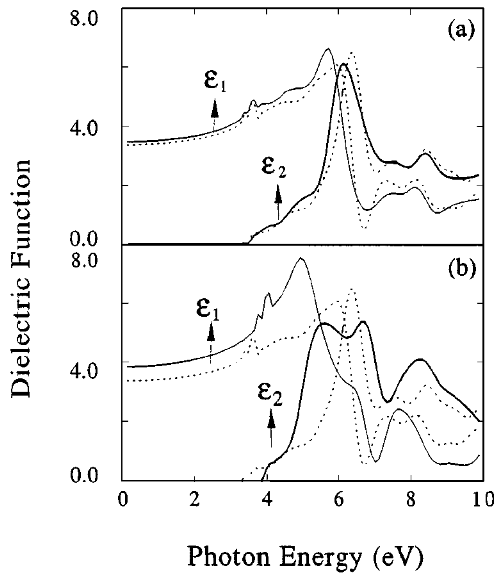

FIG. 7. The imaginary and real parts of the dielectric function of α-GaN under strains of (a) 1% and (b) 4%. The dotted lines indicate the results without strains.

Figures 8 and 10 show the refractive index (n) and reflectivity (R) with strains of (a) -1%, (b) 1%, and (c) 3%, respectively. The dotted curves are unstrained results. It can be concluded that the position of the highest peak of both n and R shifts successively to the lower-energy part with the increase of the strains, and the strains also shift the position and relative strengths of the other two little peaks. Reflectivity (R) has been measured by prior researchers,[23] whose result is compared with ours in Fig. 9. It can be seen that our result agrees quite well with the experiment.

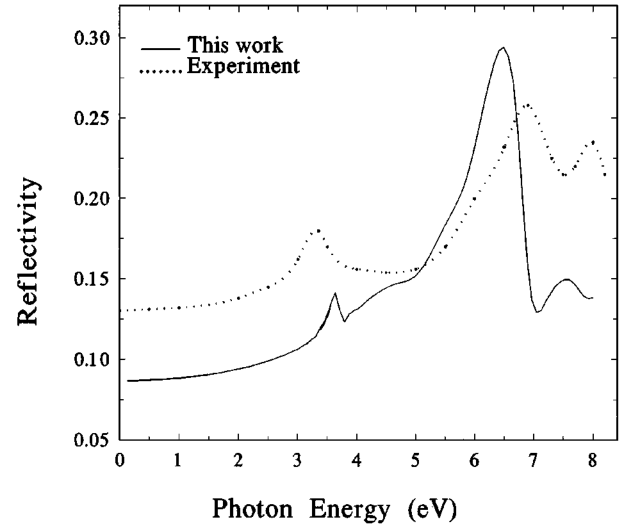

FIG. 9. Reflectivity (R) of α-GaN compared with experiment by Logothetidis *et al.*

IV. CONCLUSION

In this work, we have reported the unstrained and strained band structure and optical properties of wurtzite GaN using a semiempirical tight-binding approach in the sp^3s^* model. The unstrained fundamental gap of α-GaN is 3.45 eV. When the absolute value of the strains increase, the gap at the Γ point grows, and the α-GaN turns out to be an indirect gap semiconductor under about 5% of the strains. So in the sight of fabrication of the blue emitting-light device, it is necessary to try to decrease strains, especially positive strains. The density of states, which is obviously affected by the strains is calculated and analyzed. There are three distinct peaks dominating the unstrained $\epsilon_2(\omega)$ spectrum that can be connected

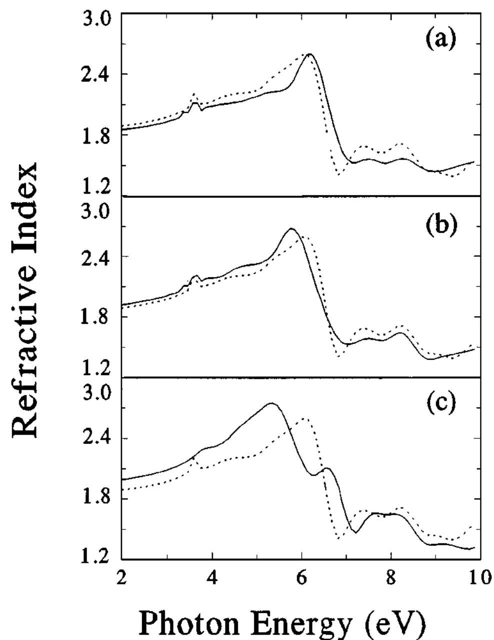

FIG. 8. Refractive index (n) of α-GaN with strains of (a) -1%, (b) 1%, and (c) 3% compared with unstrained results (dotted lines).

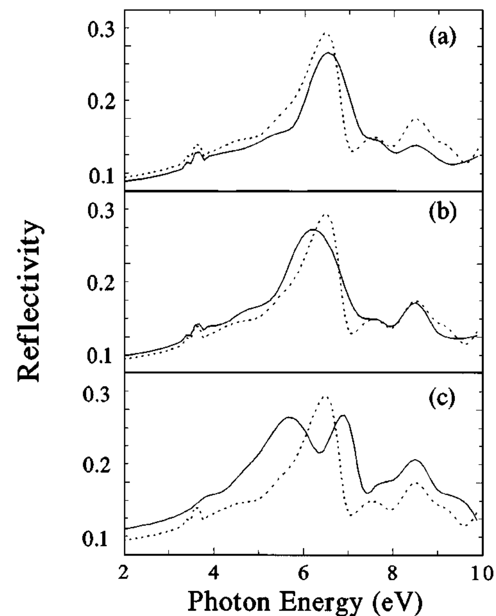

FIG. 10. Reflectivity (R) of α-GaN under strains of (a) -1%, (b) 1%, and (c) 3% compared with unstrained refractive index (n) (dotted lines).

with the band traditions of the specific points in the BZ. The position of the highest peak of $\epsilon_2(\omega)$ shifts to the low-energy part under -4%-4% strains. The refractive index, reflectivity, and the effects of strains on them are all researched in the paper, which may be very useful in the making of a photoelectric device of α-GaN in the future.

ACKNOWLEDGMENTS

The authors gratefully acknowledge the encouragement of Professor Xide Xie, Kaiming Zhang, and Xun Wang during the course of this work. The work is supported by the National Natural Science Foundation of China.

[1] R. F. Davis, Physica B **185**, 1 (1993).
[2] J. S. Foresi and T. D. Moustakas, Appl. Phys. Lett. **62**, 2859 (1993).
[3] M. Asif Khan, J. N. Kuznia, D. T. Olson, J. M. Van Hove, M. Blasingmae, and L. F. Reitz, Appl. Phys. Lett. **60**, 2917 (1992).
[4] I. Akasaki, A. Amano, N. Koide, M. Kotaki, and K. Manabe, Physica B **185**, 428 (1993).
[5] T. D. Moustakas, T. Lei, and R. J. Molnar, Physica B **185**, 36 (1993).
[6] C. J. Sun and M. Razeghi, Appl. Phys. Lett. **63**, 973 (1993).
[7] S. Bloom, G. Harbeke, E. Meier, and I. B. Ortenburger, Phys. Status Solidi B **66**, 161 (1974).
[8] H. Okumura, S. Misawa, and S. Yoshida, Appl. Phys. Lett. **59**, 1058 (1991).
[9] M. E. Lin, B. N. Sverdlov, and H. Morkoc, Appl. Phys. Lett. **63**, 3625 (1993).
[10] M. Z. Huang and W. Y. Ching, J. Phys. Chem. Solids **46**, 977 (1985).
[11] S. J. Jenkins, G. P. Srivastava, and J. C. Inkson, J. Phys. Condens. Matter **6**, 8781 (1994).
[12] K. Miwa and A. Fukumoto, Phys. Rev. B **48**, 7897 (1993).
[13] A. Rubio, J. L. Corkill, M. L. Cohen, E. I. Shirley, and S. G. Louie, Phys. Rev. B **48**, 11 810 (1993).
[14] P. Vogl, H. P. Hjalmarson, and J. D. Dow, J. Phys. Chem. Solids **44**, 365 (1983).
[15] J. C. Slater and G. F. Koster, Phys. Rev. **94**, 1498 (1954).
[16] O. Madelung, M. Schulz, and H. Weiss, in *Semiconductors*, edited by O. Madelung, Landolt-Börnstein, New Series, Group III, Vol. 17a (Springer-Verlag, Berlin, 1982).
[17] J. Arriaga, M. C. Muñoz, V. R. Velasco, and F. G. Moliner, Phys. Rev. B **43**, 9626 (1991).
[18] W. A. Harrison, in *Electronic Structures and the Properties of Solids*, edited by P. Renz and K. Sargent (Freeman, San Francisco, 1980).
[19] N. E. Christensen and I. Gorczyca, Phys. Rev. B **50**, 4397 (1994).
[20] G. Gilat and L. J. Raubenheimer, Phys. Rev. **144**, B390 (1966).
[21] H. Ehrenreich and H. R. Philips, Phys. Rev. **128**, 1622 (1962).
[22] L. C. Lew Yan Voon and L. R. Ram-Mohan, Phys. Rev B **47**, 15 500 (1993).
[23] S. Logothetidis, J. Petalas, M. Cardona, and T. D. Moustakas, Phys. Rev. B **50**, 18 017 (1994).
[24] I. Gorczyca and M. E. Chistensen, Solid State Commun. **80**, 335 (1991).
[25] Y. N. Xu and W. Y. Ching, Phys. Rev. B **48**, 4335 (1993).
[26] C. Priester, G. Allen, and M. Lannoo, Phys. Rev. B **37**, 8519 (1988).
[27] P. Perlin, I. Gorczyca, N. E. Christensen, I. Grzegory, H. Teisseyre, and T. Suski, Phys. Rev. B **45**, 13 307 (1992).